



Paper Type: Original Article

Experimental and Numerical Analysis of Annealing Effects in the Incremental Forming Process of Al1050 Aluminum Sheets

Behzad Soltani¹ , Javad Rezaei Heydari^{2,*}

¹ Department of Mechanical Engineering, University of Kashan, Kashan, Iran; bsoltani@kashanu.ac.ir.

² Department of Mechanical Engineering, University of Kashan, Kashan Iran; Javad.rezaei1368@gmail.com.

Citation:

Received: 24.04.2025

Revised: 26.06.2025

Accepted: 30.06.2025

Soltani, B., & Rezaei Heidari, J. (2025). Experimental and numerical analysis of annealing effects in the incremental forming process of Al1050 aluminum sheets. *Karshi multidisciplinary international scientific journal*, 2(2), 86-101.


Abstract


In this study, the effects of annealing and key process parameters on the incremental forming of Al1050 aluminum sheets were investigated. By varying parameters such as tool rotational speed, tool feed rate, and vertical step size, the aim was to enhance the incremental sheet forming of a truncated pyramid with a rectangular base. Numerical simulations were carried out using Abaqus software, and experimental tests were also conducted. The results showed that the T4 annealing process reduced sheet damage by 24% and significantly decreased cracking after 15 mm of stretching compared to non-annealed samples. Moreover, lower values of tool rotational speed, feed rate, and vertical step size led to improved forming quality of the workpiece.


Keywords: Annealing, Incremental forming, Finite element Simulation, Al1050 aluminum, T4 heat treatment.

1|Introduction

In the modern era, global industries are increasingly in need of novel methods to accelerate and enhance manufacturing processes. These improvements can lead to increased productivity, reduced material waste, and decreased equipment wear. One of the most critical processes in manufacturing industries related to alloy sheets

 Corresponding Author: bsoltani@kashanu.ac.ir

 <https://doi.org/10.22105/kmisj.v2i2.90>

 Licensee System Analytics. This article is an open-access article distributed under the terms and conditions of the Creative Commons Attribution (CC BY) license (<http://creativecommons.org/licenses/by/4.0>).

is forming processes. Incremental sheet forming (ISF) is an advanced metal forming technique, wherein a sheet is gradually transformed into the final product through small, incremental deformations. Research has shown that this method can be applied not only to metal sheets but also to polymeric and composite sheets.

The process is performed using a rounded-tip tool, which comes in various diameters depending on the application, and is typically connected to a CNC machine or a robotic arm. This tool gradually penetrates the sheet and follows the contour of the desired part, completing the forming process incrementally. Based on the number of contact points between the tool, sheet, and die (if any), incremental sheet forming can be classified into different types. The term *Single-Point Incremental Forming* (SPIF) is used when the opposite side of the sheet is supported by a backing plate, while *Two-Point Incremental Forming* (TPIF) is applied when a full or partial die supports the sheet [1].

The forming of aluminum and the annealing process have been subjects of significant research and practical interest in recent years. In the study by Vilundas et al. [2], the effect of annealing on the changes in Young's modulus of aluminum 1050 series sheets was investigated. Additionally, the variations in Young's modulus and Poisson's ratio of AA 2024 alloy under T4 and T65 annealing conditions were also studied. This research measured the elastic constants using ultrasonic techniques for AA 2024 and tensile testing for AA 1050. The results indicated that the variation in Young's modulus for the 1050 alloy was about 6–8%, and for the 2024 alloy, a minimal change (about 3%) was observed between the annealed and quenched conditions.

The study by Casemano and Bora[3] examined the effect of cold rolling and annealing time on the fatigue crack propagation behavior of AA 1050 aluminum alloy. Furthermore, the researchers analyzed the microstructural changes resulting from cold rolling and annealing using optical microscopy. The results showed that increasing the amount of rolling during cold rolling led to highly elongated grains in the material's microstructure. Additionally, the annealing process resulted in recrystallization and uniform grain structure. Fatigue behavior analysis demonstrated that the fatigue life of the material significantly decreased with an increase in the cold rolling percentage. In contrast, increasing the annealing time significantly enhanced the fatigue life and improved the mechanical properties.

The study by Irinah Omar et al. [4] focused on the challenges of cold spraying ceramic materials. Due to the need for plastic deformation of the feedstock particles to adhere to the substrate, cold spraying of hard and brittle ceramics such as TiO_2 faces significant challenges. Although previous studies reported the feasibility of cold spraying pure TiO_2 , the bonding mechanisms between cold-sprayed TiO_2 and the substrate were not fully understood.

The aim of this study was to investigate the relationship between oxide layer thickness, substrate deformation, and the adhesion strength of TiO_2 coatings under different conditions. Experiments were conducted using annealed AL 1050 aluminum sheets sprayed with TiO_2 powder at various temperatures. The results revealed that increasing the substrate temperature from room temperature to 400°C led to a reduction in the adhesion strength of the coatings. In this study, metallurgical bonding was identified as the main mechanism of adhesion between the TiO_2 particles and the annealed AL 1050 substrate.

In the research by Sasan Sattarpanah et al.[5], AL 1050 aluminum sheets were processed through accumulative roll bonding (ARB) for five passes. Various tests, including uniaxial tensile tests, were conducted to precisely evaluate the mechanical properties and microstructure of the material. The results demonstrated that the elongation of the annealed specimens increased by about 50%, equivalent to 2.5 times the elongation after the fifth ARB pass (20%).

The tensile strength of the annealed samples increased from 50 MPa in the initial state to 250 MPa after five passes of accumulative rolling, indicating a fivefold increase. Furthermore, the yield stress of the annealed samples was measured at 40 MPa, which is 4.5 times lower than the 180 MPa observed in the samples processed after five passes of accumulative rolling.

To evaluate the hardness of the samples, a Vickers microhardness test was performed. The results showed that the hardness of the annealed samples was 39 HV, while the hardness of the samples after the final pass of accumulative rolling was 68 HV, indicating a 1.8-fold increase in hardness. In addition, fractography tests were conducted on fractured samples following tensile tests to identify and analyze the fracture mechanisms and modes. Study by Sara George et al.[6]

In this study, the effect of rolling the AA 1050 aluminum alloy at extremely low temperatures (liquid nitrogen) was investigated. The drastic reduction in temperature during this process minimized the occurrence of dynamic

recovery. This led to substantial energy storage within the material and an increased dislocation density, which directly provided the material with high mechanical strength.

In the second part of the research, the recovery and recrystallization processes during post-rolling annealing were studied. The results showed that the dislocation structure formed during the rolling process directly affected the microstructural evolution after deformation. Moreover, during the annealing process, the reduced rolling temperature increased the driving force for recrystallization. Materials rolled at extremely low temperatures exhibited a higher number of nucleated grains, resulting in a finer microstructure after recrystallization. Study by Yazhou Liu et al. [7]

This research investigated the effect of different annealing temperatures on the microstructural evolution of Cu-Al clad sheets. The sheets were prepared using a roll-casting process, and microstructural analyses were carried out using scanning electron microscopy (SEM), transmission electron microscopy (TEM), and X-ray diffraction (XRD).

The results indicated that the increase in annealing temperature significantly affected the bonding strength of the clad sheets. Initially, the bonding strength increased with the rise in annealing temperature, but it subsequently decreased at higher temperatures. Between 250°C and 300°C, during three hours of annealing, an intermetallic compound (CuAl_2) formed at the interface of the sheets. This intermetallic compound enhanced the diffusion of copper elements and improved the bonding strength. Study by Li Feng et al. [8]

In this study, the effect of the annealing process on the microstructure and mechanical properties of Al-10Mg alloy during cold rolling was investigated. Analyses were performed using X-ray diffraction (XRD), scanning electron microscopy (SEM), electron backscatter diffraction (EBSD), and tensile tests.

The results showed that supersaturated magnesium precipitated along the grain boundaries and deformation bands during the annealing process. Furthermore, it was found that the size of the precipitates and the concentration of magnesium atoms in the solid solution increased with the annealing temperature. These findings highlight the critical role of annealing temperature in controlling the mechanical behavior and microstructure of the alloy. Study by Rezaei et al. [9]

This research studied the microstructural evolution and mechanical properties of the Al 1050 alloy during annealing and accumulative roll bonding (ARB) processes. Field emission scanning electron microscopy (FESEM) revealed that the distribution of particles within the matrix was uniform and random, and that strong mechanical bonding at the interface between the matrix and particles was achieved during the final ARB cycles.

Annealing improved the mechanical properties of the Al 1050 alloy and facilitated its machinability. Additionally, the Al 1050 alloy, classified as a wrought alloy, is typically not used in casting processes. Its high electrical conductivity, corrosion resistance, and good performance are among its notable features. Moreover, Al 1050 is widely used in heat sink manufacturing due to its high thermal conductivity [10]. Compared to other alloyed metals, Al 1050 exhibits lower mechanical strength [11]. Most previous studies have focused on processes such as cold spraying and cold rolling, while studies related to annealing using the T4 technique and incremental forming are less frequent.

Annealing Process of 1050 Aluminum Alloy. Annealing of the 1050 aluminum alloy is typically carried out at temperatures around 350°C (662°F). Among the available methods, the T4 heat treatment process is commonly used for this alloy. In general, heating and cooling cycles in aluminum alloys are classified within the T-series treatments [12].

In the T4 process, the alloy is heated to a temperature range between 350°C and 370°C, followed by air cooling. This procedure stabilizes the alloy's mechanical and microstructural characteristics, enabling improved performance during subsequent forming operations [13].

The principal objective of annealing Al 1050 is to enhance its formability. Without annealing, forming operations can result in cracking, tearing, or other forms of material degradation. Annealing significantly mitigates these risks, improving the alloy's ductility and reducing residual stresses [14].

Research on AL 1050 Alloy and Incremental Forming. In this study, annealing operations were performed on AL 1050 alloy sheets, followed by incremental sheet forming into a truncated rectangular pyramid shape. The effect of annealing on mechanical properties, particularly formability, was investigated and compared both numerically and experimentally for annealed and non-annealed sheets.

All numerical simulations related to this research were conducted using Abaqus software. It should be noted that during the annealing process, the temperature was kept constant and followed the T4 method (350°C to 370°C).

2| Numerical Simulation

The commercial finite element software ABAQUS was used to model the incremental sheet forming process. In this modeling, surface-to-surface contact was defined with a friction coefficient of 0.1 based on the Coulomb friction model. High-accuracy quadrilateral elements were used for meshing, and a total of 25,280 elements were considered for simulating the sheet.

In the sheet modeling, first-order four-node shell elements (S4R) were used in an explicit solution. In the interaction section, the contact between the sheet and the tool was defined as surface-to-surface contact. Additionally, the initial and final parts of the die were tied to the four edges of the sheet. These parts in the tool were constrained using rigid body constraints.

Geometry of the Aluminum Sheet (Figure1). In Figure 1, a side view of a truncated rectangular pyramid is depicted from both horizontal and vertical angles. This figure illustrates the final geometry of the AL 1050 aluminum sheet after the forming process in this study. The blue arrows in the image indicate the wall radius of the pyramid, which is the same for both the horizontal and vertical views. This geometry provides an accurate representation of the sheet's deformation during the incremental forming process.

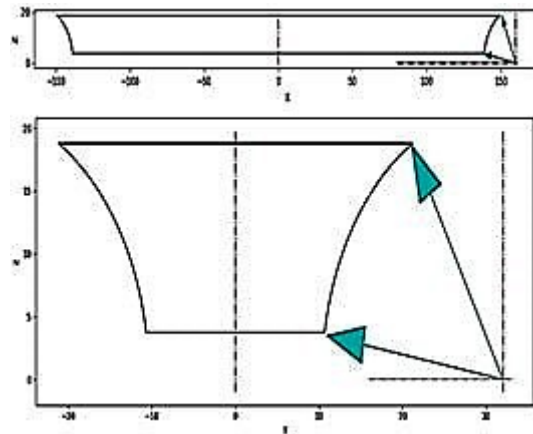


FIGURE 1. Dimensions and coordinates of points on the wall of the pyramid.

Geometry of Related Parts (Figure2).

- **Figure 2(a):** This section represents the geometry of the clamping plate, designed as a die positioned above the sheet. The aluminum sheet is clamped to this die using holding clamps.
- **Figure 2(b):** This part shows the bottom plate placed beneath the aluminum sheet, with a height of 15 mm.
- **Figure 2(c):** This section illustrates the geometry of the intended aluminum sheet. The sheet dimensions are detailed in Figure 1, and this image complements the geometric design information.

3| Simulation Settings

Figure 2:

- (a) Holding plate with a thickness and fillet of 3 mm (designed as Solid Extrude - Rigid Body).
- (b) Bottom plate under the sheet with a thickness of 3 mm (designed as Solid Extrude – Rigid Body).
- (c) Aluminum sheet with a thickness of 1 mm (designed as Solid Extrude - Deformable).

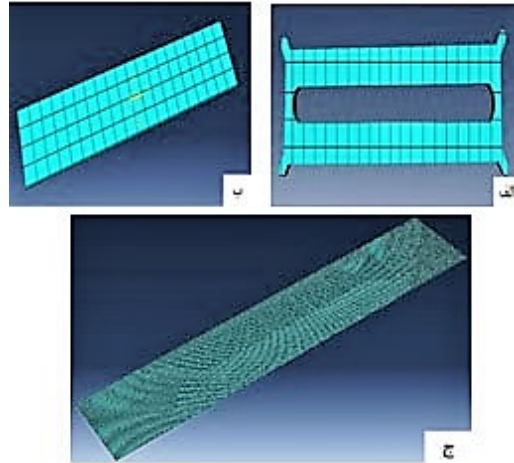


FIGURE 2. Geometry of related parts: (a) clamping plate, (b) bottom plate, (c) aluminum sheet.

The stress-strain properties of Al1050 aluminum are also shown in Figure 3.

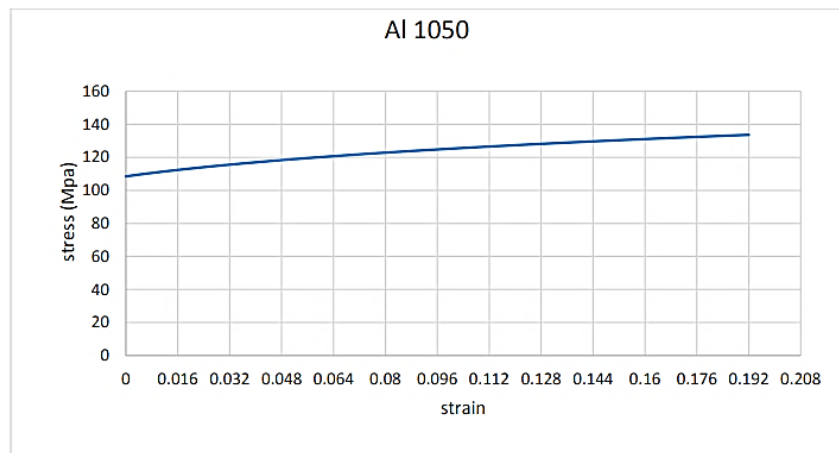


FIGURE 3. Stress-strain properties of Al1050 aluminum.

Definition of Stops and Simulation Settings. One of the key aspects of the simulation process is the definition of stops, which was previously addressed for calculating the toolpath. At this stage, the required time for each stop is determined; therefore, the tool feed rate is of great importance.

In the first phase of the tests, the initial tool feed rate was set at 16.67 mm/s. The required time for each segment of the toolpath was calculated by dividing the path length by the feed rate, and this time was assigned to each stop.

To improve the efficiency and performance of the simulation, a mass scaling factor of 40 was applied, which plays a significant role in optimizing the computations.

Toolpath and Punch Geometry. The toolpath used in this study for the forming process is shown in Figure4. The figure also shows the geometry of the tool (punch), which is designed as a sphere with a radius of 5 mm.

As shown in the figure, as the step depth increases, the distance between steps decreases. This design adjustment was made to reduce the stresses applied to the sheet and to improve its mechanical behavior during the thickness reduction phase.

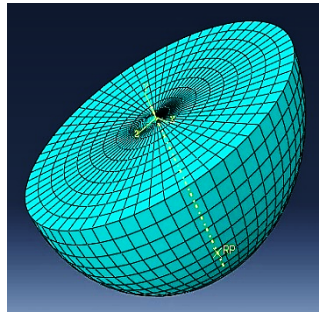


FIGURE 4. Tool with a 5 mm radius (designed as Shell Revolve - Rigid Body).

Numerical Simulation Results of the Unannealed Sheet. In this study, the numerical simulations were successfully completed, and nine runs were performed considering the necessary modifications for each simulation. The average execution time for each simulation was approximately 10 hours. To achieve optimal values for various parameters, including the tool position, the tool rotational speed, and the feed rate, multiple calibrations were carried out.

Figure[fig:finalforming] shows the final forming result of the unannealed aluminum sheet with a depth of 15 mm from different perspectives. During the forming process, the stress at all points remained below the allowable stress limit. However, despite the good formability of the pyramid along the tool path, a bulging was observed at the center of the pyramid due to the applied pressure and the long cross-sectional length. This defect cannot be corrected with the current tool path, and thus a new tool path design will be required in the next step to eliminate this issue.

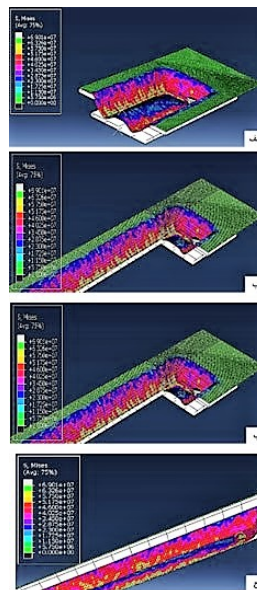


FIGURE 5. (a) Horizontal section of the unannealed sheet along the (x) -axis, (b) Section of the unannealed sheet along the (x) - and (y) -axes, (c) Bottom view of the formed sheet, (d) Vertical cross-sectional view parallel to the sheet direction.

Thickness Variation of the Unannealed Sheet. In the conducted simulation, it was observed that the minimum thickness variation occurred at the center and edges of the sheet (areas not subjected to the forming process). The greatest thickness reduction was observed in the wall section close to the bottom of the pyramid-shaped container. The stress and strain of one of the elements at the base section of the pyramid from the beginning to the end of the operation are shown in Figure [fig:fig6]. The applied stress was lower than the yield stress of the Al 1050 alloy; therefore, the reference stress was considered as the yield stress.

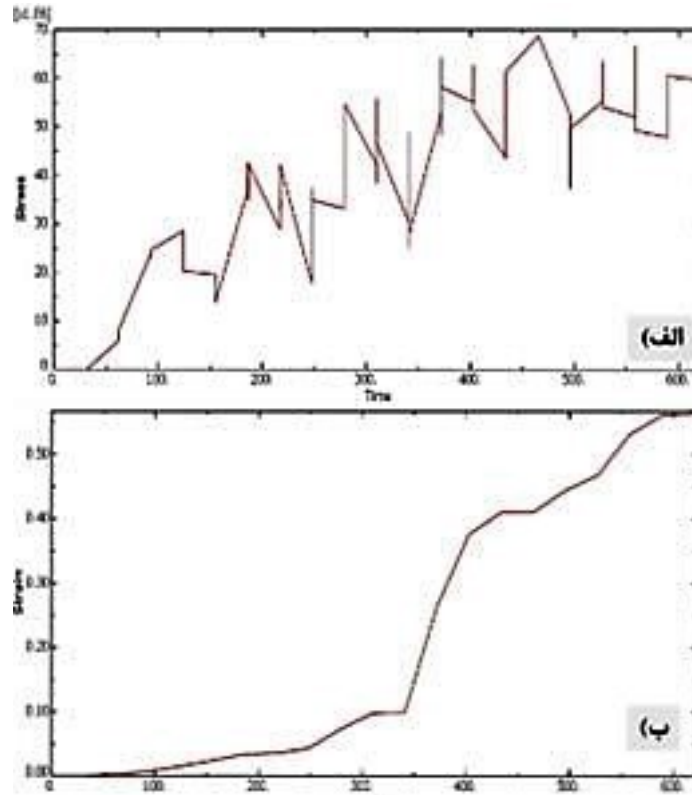


FIGURE 6. (a) Stress of a sample element at the base section of the pyramid, (b) Strain of a sample element at the base section of the pyramid.

Moreover, the displacement of one of the wall elements of the pyramid from the beginning to the end of the operation is shown in Figure 7. Based on the results, the displacement along the x -axis is negligible, which ideally should be zero. The displacement along the y -axis initially increases slightly due to the stretching of the sheet, but eventually decreases. The displacement along the z -axis is decreasing overall; however, in some cases, the depth formed is reduced, causing the sheet to rebound upwards.

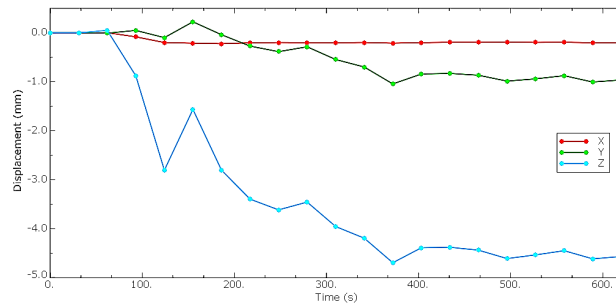


FIGURE 7. Displacement of a sample element at the wall of the pyramid.

Stress and Strain Analysis in the Pyramid Wall. The stress and strain of one of the elements at the wall section of the pyramid from the beginning to the end of the operation are shown in Figure 8. During the simulation process, it was observed that whenever the stress exceeded the yield stress, plastic strain occurred. After approximately 200 seconds, the strain started to oscillate and eventually reached 40%.

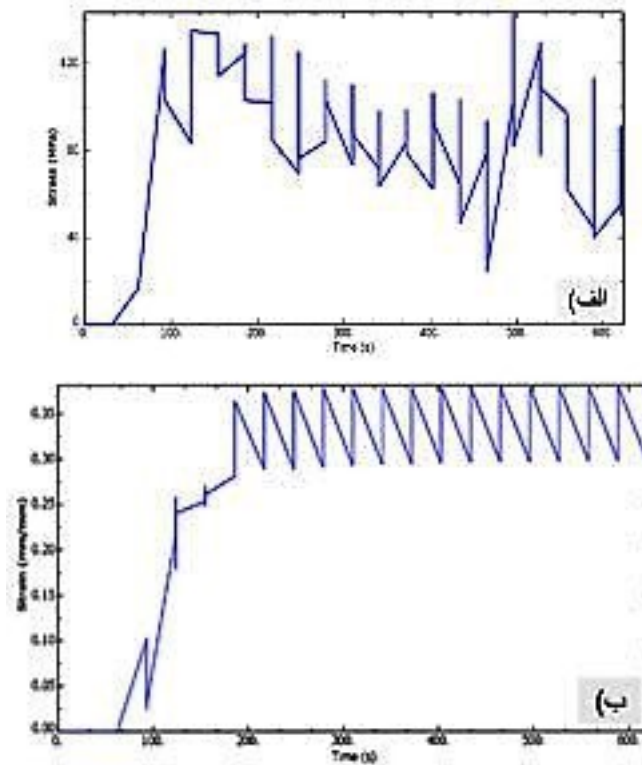


FIGURE 8. (a) Stress applied to a sample element at the pyramid wall, (b) Strain of a sample element at the pyramid wall.

Numerical Simulation Results of the Annealed Sheet. Next, by changing the material of the sheet to annealed aluminum 1050 series, the simulation was conducted and the corresponding results were extracted. In this phase of the simulations, nine successful runs were completed, with an average simulation time of approximately 11 hours, considering necessary modifications. Multiple runs were performed to achieve calibrated positioning in the simulations.

In many cases, the sheet experienced rupture (cracking), but after calibration, these issues were significantly reduced. Initially, the tool speed was set similar to the previous section; however, due to the inappropriate speed, the sheet exhibited excessive cracking and distortion. Therefore, approximately 14 runs were performed to determine a reliable range for the simulation variables.

The mechanical properties of the annealed aluminum 1050 series, used as input data for the software, were obtained from the study by Sępkowska et al. [ref15], which also employed the T4 method.

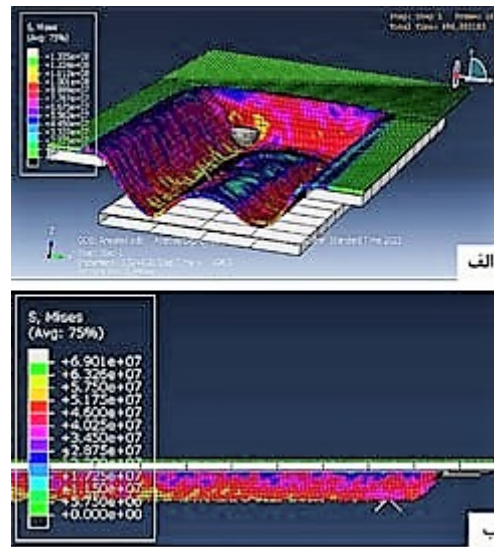


FIGURE 9. Final forming result of the annealed aluminum 1050 series sheet with a depth of 15 mm.

As can be seen, despite the good formability of the pyramid along the tool path, a bulging is observed at the center of the pyramid due to the applied pressure and the long cross-sectional length. This defect cannot be corrected with the current tool path, and thus a new tool path design will be required in the next step to eliminate this issue.

The stress and strain of one of the elements of the pyramid base section of the annealed sheet from the beginning to the end of the process are shown in Figure[fig:stressstrain1]. Throughout the forming operation, it was found that the stress values at various points remained below the allowable stress.

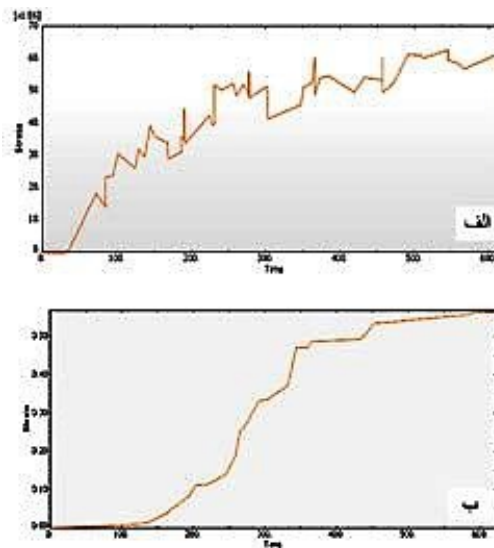


FIGURE 10. (a) Stress of a sample element in the bottom section of the pyramid-shaped annealed sheet. (b) Strain of a sample element in the bottom section of the pyramid-shaped annealed sheet.

Stress and Strain Analysis at the Pyramid Base of the Annealed Sheet. The stress and strain of one of the elements of the pyramid base of the annealed sheet from the beginning to the end of the process are shown in

Figure [fig:stressstrain1]. Throughout the forming process, it was observed that the stress values at different points remained below the allowable limits.

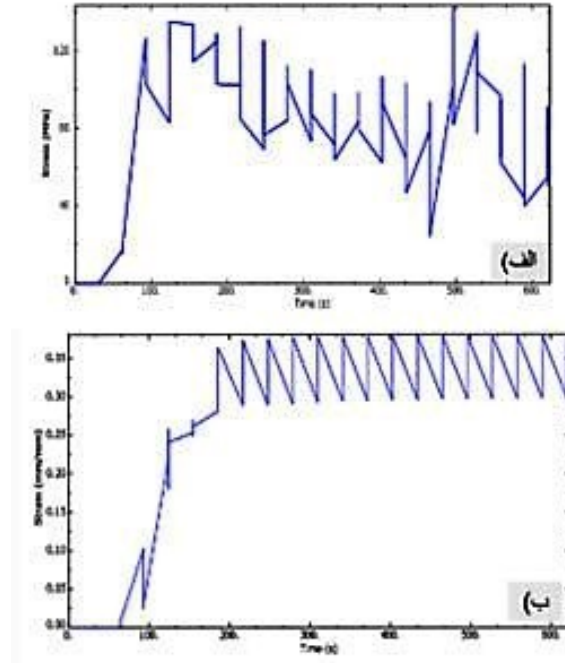


FIGURE 11. (a) Stress applied to a sample element in the wall section of the annealed pyramid. (b) Strain of a sample element in the wall section of the annealed pyramid.

Simulation of the Springback in Incremental Sheet Forming. At this stage, the springback process was simulated by calculating the horizontal distance, the radius of the pyramid wall, the time of each step, the tool path, the step height, and the coordinates. The stress at the end of the incremental forming process on the pyramid walls and the residual stress after stress release during the springback process are shown in Figures [fig:stressstrain3](a) and (b), respectively.

The maximum stress values observed in Figures [fig:stressstrain3](a) and (b) were 4.612×10^8 and 3.140×10^8 respectively. Furthermore, the amount of springback in the pyramid walls was measured as 1.8 mm.

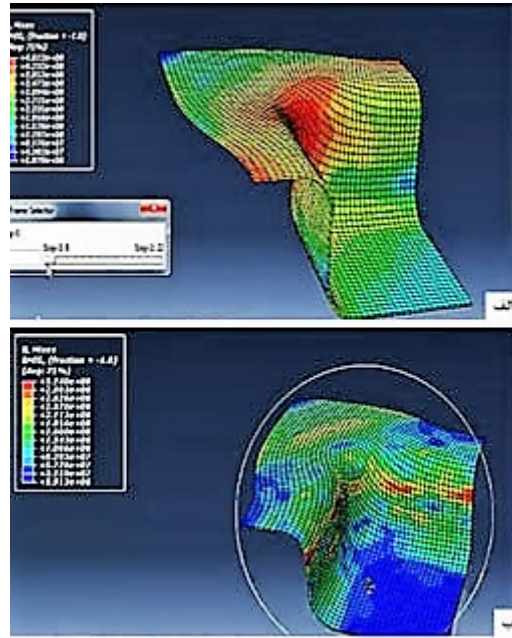


FIGURE 12. (a) Stress at the end of the incremental sheet forming process on the pyramid walls. (b) Residual stress after stress release at the end of the springback process.

4| Experimental Tests

At this stage, 450×80 mm sheets were prepared from a 100×100 cm 1050 series aluminum sheet according to the part design. Then, from six small sheets (three pairs) obtained, three sheets were annealed at 350°C for one hour using the T4 method in a furnace and subsequently cooled in ambient air. These sheets (Figure [fig:13]) showed visible discoloration, and the difference in hardness between annealed and unannealed sheets was clearly noticeable.

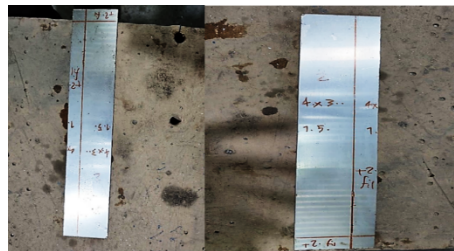


FIGURE 13. A sample of an annealed sheet.

Forming Tool Used. The selected tool (Figure [fig:14]) was made of plain high-speed steel, with a length of 200 mm and a diameter of 10 mm. Its tip was ground into a spherical shape with a radius of 5 mm using a sharpening process.



FIGURE 14. Image of the tool after forming.

Die Used. In the next step, iron plates with a thickness of 20 mm (as shown in Figure [fig:15]) were used as dies. These plates were first cut using an air cutter, then measured, and finally machined into the final shape using a CNC milling machine.



FIGURE 15. Image of the die after CNC machining processes.

Experimental Results. After designing the tool paths and related drawings in PowerMILL software, the command codes were transferred to the machine, and the parts were placed in the device. In total, three annealed and three unannealed sheets were tested. Each sheet forming process took between 60 and 90 minutes. The experiments started with a feed rate of 16.60 mm/s, a vertical step of 0.5 mm, and a spindle rotational speed of 1500 rpm. Then, by changing the parameters of feed rate, spindle speed, and vertical step, the results were extracted and are fully presented in Table [tab:1] and Figure [fig:16].

Ultimately, it was found that by adjusting forming parameters — specifically by reducing the rotational speed, feed rate, and vertical step — complete forming was achieved in the third sample. Overall, the results indicated that lowering the feed rate and rotational speed, combined with smaller vertical steps, significantly improves the incremental forming quality of the 1050 aluminum sheet.

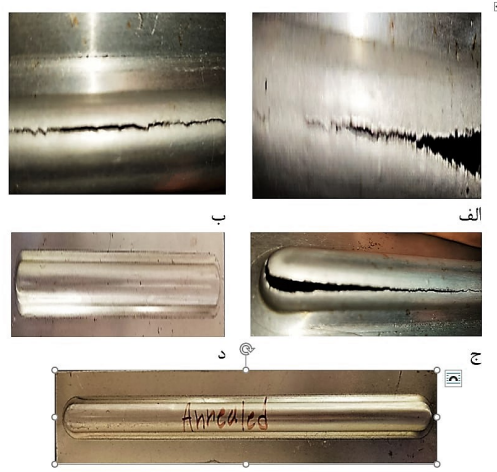


FIGURE 16. (a) Crack formation in the center of the sheet after 8 mm stretching. (b) Cracking on one side of the sheet. (c) Severe cracking in the right corner after 10 mm stretching. (d) Desired geometry obtained from the unannealed sheet. (e) Desired geometry obtained from the annealed sheet.

Experimental Thickness Variations. In examining the thickness changes of annealed and unannealed samples, it was found that with increasing stretching of the workpiece, thickness reduction became more pronounced.

- In the first series of samples, after forming, the annealed sample showed a thickness reduction of 0.2 mm, and the unannealed sample showed a reduction of 0.15 mm in the pyramid walls.
- In the second series of samples, the thickness reduction was 0.32 mm for the annealed and 0.23 mm for the unannealed samples.
- In the third series of samples, the thickness reduction reached 0.38 mm for the annealed and 0.3 mm for the unannealed samples.
- The highest thickness reduction occurred in the fourth series, with reductions of 0.41 mm for the annealed sample and 0.38 mm for the unannealed sample.

Overall, it was found that annealed samples exhibited greater thickness reduction compared to unannealed ones. This greater reduction indicated better formability and higher deformation capability of the annealed samples.

Experimental Springback. In this phase, the springback was experimentally determined according to Table[tab:2].

TABLE 1. Experimental Springback Values.

Sample	Springback Amount
Unannealed Sample 1	3.6978
Annealed Sample 1	2.3981
Unannealed Sample 2	3.6039
Annealed Sample 2	2.3562
Unannealed Sample 3	3.5264
Annealed Sample 3	2.3482

5| Results and Discussion

By comparing the results of the simulation and experimental sections according to the charts in Figures 17 to 19, it was observed that in sample No. 1, the vertical force changed midway through the tool path, and the material showed significant resistance to deformation. This resistance caused the annealed sample to crack in the middle section, while the unannealed sample experienced cracking from the beginning to the end.

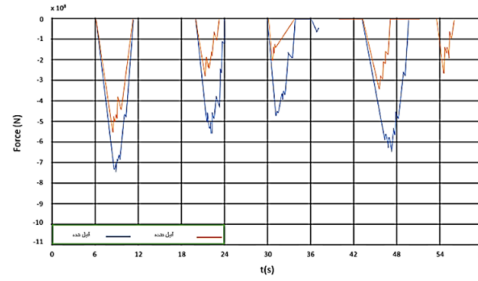


FIGURE 17. Diagram for annealed and unannealed samples No. 1, with a feed rate of 16.6 mm/s and spindle speed of 1500 rpm, experimentally measured at the pyramid wall cross-section.

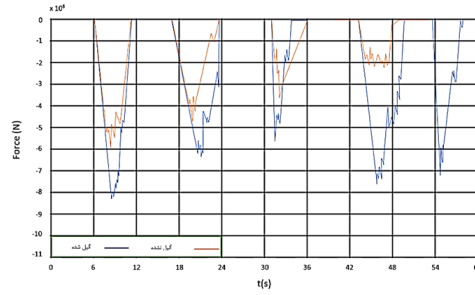


FIGURE 18. Diagram for annealed and unannealed samples No. 2, with a feed rate of 12 mm/s and spindle speed of 1250 rpm, experimentally measured at the pyramid wall cross-section.

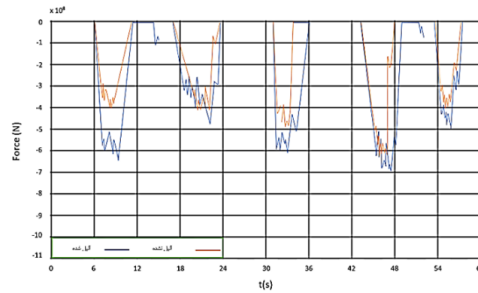


FIGURE 19. Diagram for annealed and unannealed samples No. 3, with a feed rate of 8 mm/s and spindle speed of 850 rpm, experimentally measured at the pyramid wall cross-section.

The error between the vertical force in the experimental and simulation results varied between 10% and 20%.

6|Conclusion

In the present study, the formability of annealed and non-annealed 1050 series aluminum sheets was investigated experimentally and numerically in the incremental forming process. In this investigation, the fracture process in the sheets was analyzed, and the effect of tool radius, vertical step size, and tool feed rate on formability was examined. The obtained results are as follows:

- The annealed 1050 series aluminum sample exhibited greater elongation compared to the non-annealed sample.
- Reducing the tool feed rate led to increased elongation in the tested samples. Additionally, decreasing the feed rate improved the forming accuracy, resulting in higher elongation.

TABLE 2. Forming Results of Three Annealed and Three Unannealed Samples

Title	Unannealed Sheet 1	Annealed Sheet 1	Unannealed Sheet 2	Annealed Sheet 2	Unannealed Sheet 3	Annealed Sheet 3
Feed Rate	16.60 mm/s	16.60 mm/s	12 mm/s	12 mm/s	8 mm/s	8 mm/s
Vertical Step	0.5 mm	0.5 mm	0.3 mm	0.3 mm	0.2 mm	0.2 mm
Rotational Speed	1500 rpm	1500 rpm	1250 rpm	1250 rpm	850 rpm	850 rpm
Drawn Depth	8 mm	11 mm	10 mm	12 mm	15 mm	15 mm
Result	Sheet cracked from the middle of the left corner and the process stopped, Fig. 16(a).	Sheet cracked from one side (left to right) and the process stopped, Fig. 16(b).	Severe cracking at the right corner, process stopped, Fig. 16(c).	Partial cracking at the middle area, process stopped.	Sheet successfully formed into the desired geometry, Fig. 16(d).	Sheet successfully formed into the desired geometry, Fig. 16(e).

- Decreasing the rotational speed of the tool from 1500 rpm to 1000 rpm increased the elongation during the forming of the samples. The appropriate rotational speed for the incremental forming of 1050 series aluminum sheets is 1000 rpm.
- Reducing the tool feed per revolution led to better quality and greater elongation in the incremental forming of the mentioned sheets. Reducing the feed from 0.5 mm per revolution to 0.2 mm per revolution resulted in less cracking of the sheets.
- Performing the annealing process on 1050 series aluminum during incremental forming can cause a reduction in thickness.
- Annealing the 1050 series aluminum workpiece can improve the incremental forming process of truncated rectangular pyramid geometries compared to non-annealed samples.

7| Acknowledgments

The authors would like to express their sincere gratitude to the editors and anonymous reviewers for their invaluable comments and constructive feedback, which significantly contributed to the enhancement of this paper.

8| Conflicts of Interest

The authors declare that there is no conflict of interest concerning the reported research findings. Funders played no role in the study's design, in the collection, analysis, or interpretation of the data, in the writing of the manuscript, or in the decision to publish the results.

References

- [1] Shi, Y., Zhang, W., Cao, J., and Ehmann, K. F. (2019). Experimental study of water jet incremental microforming with supporting dies. *Journal of Materials Processing Technology*, 268, 117–131. <https://doi.org/10.1016/j.jmatprotec.2019.01.012>
- [2] Villuendas, A., Roca, A., and Jorba, J. (2007). Change of Young's modulus of cold-deformed aluminum AA 1050 and of AA 2024 (T65): a comparative study. *Materials Science Forum*, 539, 293–298. <https://www.scientific.net/msf.539-543.293>
- [3] Kusmono, K., Bora, C., and Salim, U. A. (2021). Effects of cold rolling and annealing time on fatigue resistance of AA5052 aluminum alloy. *International Journal of Engineering*, 34(9), 2189–2197. <https://doi.org/10.5829/ije.2021.34.09c.16>
- [4] Omar, N. I., Yamada, M., Yasui, T., and Fukumoto, M. (2020). Influence of annealed aluminum properties on adhesion bonding of cold sprayed titanium dioxide coating. *In Material Flow Analysis*, IntechOpen. <https://doi.org/10.5772/intechopen.94097>
- [5] Sattarpanah Karganroudi, S., Hatami Nasab, B., Rahmatatabadi, D., Ahmadi, M., Delshad Gholami, M., Kasaeian-Naeini, M., Hashemi, R., Aminzadeh, A., and Ibrahim, H. (2021). Anisotropic behavior of Al1050 through accumulative roll bonding. *Materials*, 14(22), 6910. <https://doi.org/10.3390/ma14226910>
- [6] George, S., and Mias, C. (2015). Effect of rolling temperature on annealing of AA1050 aluminium alloy. *Materials Science Forum*, 828, 200–205. <https://doi.org/10.4028/www.scientific.net/MSF.828-829.200>
- [7] Liu, Y., Wang, W., Huang, Y., Liu, J., Xie, J., Guo, L., Zhang, M., and Volinsky, A. A. (2019). Effect of annealing temperature on microstructure and bond strength of cast-rolling Cu–Al clad plates. *Materials Research Express*, 6(8), 086556. <https://doi.org/10.1088/2053-1591/ab1d3a>

-
- [8] Feng, L., Li, J., Huang, C., and Huang, J. (2019). Annealing response of a cold-rolled binary Al–10Mg alloy. *Metals*, 9(7), 759. <https://doi.org/10.3390/met9070759>
- [9] Rezayat, M., and Akbarzadeh, A. (2012). Fabrication of aluminium matrix composites reinforced by submicrometre and nanosize Al_2O_3 via accumulative roll bonding. *Materials Science and Technology*, 28(11), 1233–1240. <https://doi.org/10.1179/1743284712Y.00000000060>
- [10] Suresh, K., Regalla, S. P., and Kotkundae, N. (2018). Finite element simulations of multi-stage incremental forming process. *Materials Today: Proceedings*, 5(2), 3802–3810. <https://doi.org/10.1016/j.matpr.2017.11.633>
- [11] Su, H., Huang, L., Li, J., Ma, F., Huang, P., and Feng, F. (2018). Two-step electromagnetic forming: A new forming approach to local features of large-size sheet metal parts. *International Journal of Machine Tools and Manufacture*, 124, 99–116. <https://doi.org/10.1016/j.ijmachtools.2017.10.005>
- [12] Yoganjaneyulu, G., Narayanan, C. S., and Narayanasamy, R. (2018). Investigation on the fracture behavior of titanium grade 2 sheets by using the single point incremental forming process. *Journal of Manufacturing Processes*, 35, 197–204. <https://doi.org/10.1016/j.jmapro.2018.07.024>
- [13] Zahedi, A., Dariani, B. M., and Mirnia, M. J. (2019). Experimental determination and numerical prediction of necking and fracture forming limit curves of laminated Al/Cu sheets using a damage plasticity model. *International Journal of Mechanical Sciences*, 153, 341–358. <https://doi.org/10.1016/j.ijmecsci.2019.02.002>
- [14] Bologaa, O., Breaz, R., and Racz, S. (2018). Evaluate the possibility of introducing single point incremental forming on industrial scale. *The International Academy of Information Technology and Quantitative Management*, 139(8), 408–416. <https://doi.org/10.1016/j.procs.2018.10.262>
- [15] Skibinska, K., Smola, G., Bialo, L., et al. (2020). Influence of annealing time of aluminum AA1050 on the quality of Cu and Co nanocones. *Journal of Materials Engineering and Performance*, 29, 8025–8035. <https://doi.org/10.1007/s11665-020-05267-8>